Atmospheric Environment 55 (2012) 425–430

Contents lists available at SciVerse ScienceDirect

Atmospheric Environment

journal homepage: www.elsevier.com/locate/atmosenv

Effect of absorbing aerosols on snow albedo reduction in the Sierra Nevada

Wei-Liang Lee [a,*], K.N. Liou [b]

[a] Research Center for Environmental Changes, Academia Sinica, Taipei, Taiwan
[b] Department of Atmospheric and Oceanic Sciences and Joint Institute for Regional Earth System Science and Engineering, University of California, Los Angeles, CA, USA

ARTICLE INFO

Article history:
Received 6 January 2012
Received in revised form
6 March 2012
Accepted 9 March 2012

Keywords:
Snow albedo
Aerosol deposition
Satellite remote sensing
Sierra Nevada

ABSTRACT

This paper investigates snow albedo changes in the Sierra Nevada Mountain area associated with potential deposition of absorbing aerosols in spring by using the snow albedo, aerosol optical depth, land surface temperature, and other relevant parameters available from the Moderate-Resolution Imaging Spectroradiometer (MODIS) onboard the NASA Terra satellite during 2000–2009. Satellite pixels with 100% snow cover have been selected to derive the monthly mean snow albedo value, along with aerosol optical depth, surface temperature, and days after snowfall in March and April to perform multiple regression analysis. We show that aerosol optical depth, which generally includes dust and black carbon over the Sierra Nevada as a result of the transpacific transport from East Asia and local sources, represents a significant parameter affecting snow albedo variation, second only to the land surface temperature change. The regression analysis illustrates that a one standard deviation increase in land surface temperature (2.2 K) and aerosol optical depth (0.044) can lead to decreases in snow albedo by 0.038 and 0.026, respectively. This study also shows that approximately 26% of snow albedo reduction from March to April over the Sierra Nevada is caused by an increase in aerosol optical depth, which has a profound impact on available water resources in California. However, the results show that there are no significant trends for snow albedo, surface temperature, and aerosol optical depth of snow-covered areas over the Sierra Nevada Mountain area in this 10-year period.

1. Introduction

The cryosphere plays an important role in the energy budget of the coupled atmosphere–land system. A slight decrease in snow albedo can significantly increase the amount of solar radiation absorbed by the surface, further reducing snow albedo. This snow albedo feedback has been considered the most significant positive amplification of the increase in global surface temperature (IPCC, 2007).

The reflection of sunlight from snow is influenced by snow impurities, time of snow aging, and surface temperature (e.g. Warren and Wiscombe, 1980; Marshall and Oglesby, 1994; Aoki et al., 2003). Snow impurities are produced by two processes: the wet deposition of aerosols in snow via precipitation and scavenging, and the dry deposition of aerosols directly onto snow fields. The wet deposition, resulting from external or internal mixing of absorbing aerosols (e.g., black carbon and dust) with snowflakes, drastically alters their optical properties and leads to snow albedo reduction (Liou et al., 2011). The dry deposition of absorbing aerosols would likewise decrease snow albedo. Both processes trap more solar flux in the land surface, and lead to snow ablation (Warren and Wiscombe, 1980; Chylek et al., 1983). Furthermore, recent studies have suggested that anthropogenic black carbon (BC) might have caused significant reductions in the extent and albedo of snow and sea ice, and that this result could be more effective than greenhouse gases in increasing surface temperature for a given forcing (e.g., Hansen and Nazarenko, 2004; Flanner et al., 2007; McConnell et al., 2007; Ming et al., 2009; Hadley et al., 2010).

The snowpack in high-elevation Sierra Nevada regions is a major source of California's water supply. The snowpack stores fresh water during the cold and wet season, and gradually releases water during the warm and dry season (Kattelmann, 1996). Model simulations have shown that the increase in aerosols could lead to a reduction in albedo of snowpack in this area (Hadley et al., 2010). The impact of albedo changes on the spring snowmelt in the Sierra Nevada region is an important concern because the amount and timing of snowmelt in this region are critical factors in determining water resources (e.g., Leung and Ghan, 1999; Kim et al., 2002; Jacobson, 2007).

The prime objective of this study is to investigate the effect of aerosols on snow albedo reduction over the Sierra Nevada during the spring season based on satellite remote sensing data from the

* Corresponding author. Tel.: +886 2 26539885x251; fax: +886 2 27833584.
E-mail address: leelupin@gate.sinica.edu.tw (W.-L. Lee).

1352-2310/$ – see front matter © 2012 Elsevier Ltd. All rights reserved.
doi:10.1016/j.atmosenv.2012.03.024

year 2000–2009. Section 2 describes the remote sensing data from MODIS aboard Terra satellite, including snow cover, snow albedo, aerosol optical depth and land surface temperature, and presents the gridded precipitation analysis data from *in situ* measurements. In Section 3, we show the evolution of snow albedo associated with aerosol optical depth, surface temperature, and time of snow aging. The multiple linear regression analysis is applied to the available datasets in order to estimate the effect of aerosol deposition on albedo reduction. Conclusions are given in Section 4.

2. Observational data

To demonstrate the snow albedo reduction over the Sierra Nevada, we selected an area with elevation greater than 1600 m located within a rectangular box from 35° to 40°N latitude and from 117° to 121°W longitude, as shown in Fig. 1. Some scattered mountains that are not part of the Sierra Nevada range are excluded. Surface topography with a 1 km resolution was taken from the HYDRO1k geographic database available from the U.S. Geological Survey (USGS) National Center for Earth Resources Observation and Science (EROS) data center (data available at http://edc.usgs.gov/products/elevation/gtopo30/hydro/index.html).

The daily fractional snow cover (Hall et al., 2002, 2012; Riggs et al., 2006) and snow albedo (Klein and Stroeve, 2002) at a 500 m resolution and the daily land surface temperature (Wan, 2012) at a 1 km resolution were obtained from the MODIS aboard the Terra satellite. The daily snow cover algorithm has been validated by Klein and Barnett (2003) with *in situ* measurement in the Upper Rio Grande River Basin, showing a high agreement of 86%. The effect of the surface slope is considered in the latest version of the algorithm, and the snow cover in mountainous areas, such as the Tibetan Plateau, has also been evaluated with an overall accuracy of 90% (Pu et al., 2007). The daily snow albedo algorithm for MODIS employed a look-up table approach for the bidirectional reflectance distribution function (BRDF) of snow modeled by the Discrete Ordinates Radiative Transfer program (DISORT, Stamnes et al., 1988). Since reflection of snow is anisotropic over non-forested surfaces, BRDFs for all potential combination of the solar and sensor zenith angles and the relative azimuth between the sun and the sensor are calculated by DISORT, while the local slope and aspect of the surface are also taken into account. For forest areas, which are identified by MODIS land cover type datasets, isotropic reflection is assumed. Snow albedo is only determined for cloud-free and snow-covered pixels identified by the MODIS cloud mask and snow cover algorithm, respectively.

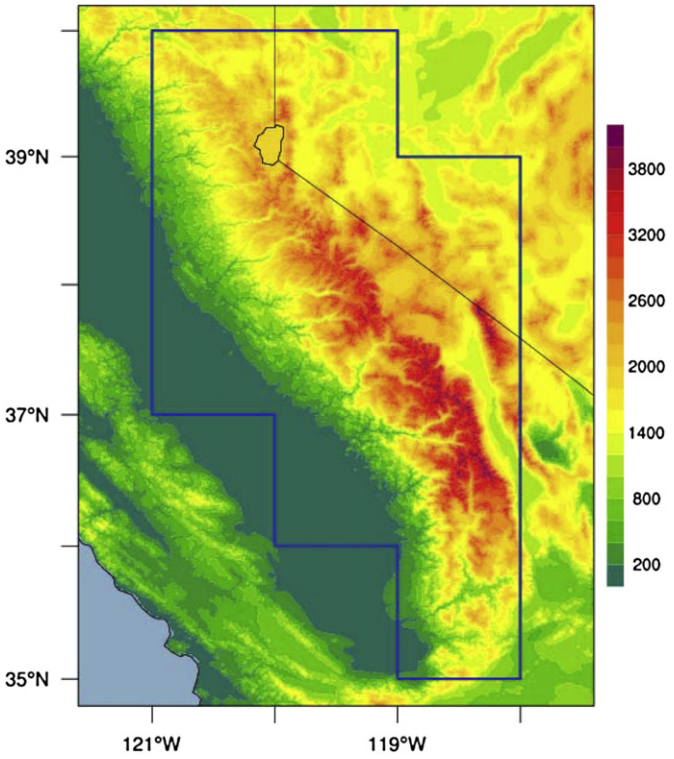

Fig. 1. Elevation map in the Sierra Nevada region. The blue box indicates the region where the monthly averages of aerosol optical depth were taken for the Sierra Nevada. (For interpretation of the references to colour in this figure legend, the reader is referred to the web version of this article.)

Our objective is to document the evolution of snow albedo in March and April. For this reason, we introduce a variable, pure snow albedo (PSA), defined as the snow albedo for pixels with 100% snow cover during the entire study period, to circumvent the contamination of snow albedo by bare land. The monthly means of PSA and land surface temperature for each snow-covered pixel were first calculated, followed by taking spatial means for these pixels. For presentation purposes, we display PSA maps for March and April for four years between 2000 and 2009, as shown in Fig. 2. As expected, mean PSA is generally higher in March, primarily due to lower temperatures, smaller aerosol optical depths, and more frequent snowfalls.

The daily aerosol optical depth (AOD) at a wavelength of 0.55 μm at a 1° resolution was also taken from MODIS/Terra dataset. The algorithm for AOD retrieval over land has been developed by Levy et al. (2007) utilizing MODIS reflectance data in the 0.47, 0.66, and 2.12 μm bands. The region covering the Sierra Nevada for monthly averages of AOD is also shown in Fig. 1. Missing data frequently occurs for daily AOD due to the presence of clouds. For this reason, to obtain the monthly mean of AOD, only the pixels with 10 or more valid values of daily AOD in the whole month were used to calculate monthly averages. If a threshold with fewer than 10 days was used, the monthly mean value would become statistically unreliable because some episodic events could significantly affect the analysis. For example, the regression coefficients differ substantially with thresholds of 9 and 8 days. When using a threshold with greater than 10 days, we find that the regression coefficients generally remain unchanged.

The composition of the deposited aerosols on snow fields remains a complicated issue. Both black carbon and mineral dust substantially darken snow, although of the two, black carbon is more effective (Liou et al., 2011). Ground measurements show that transpacific Asian dust aerosols are the primary component in the total aerosol mass over the high-elevation regions in the Western United States (VanCuren, 2003; VanCuren et al., 2005). Since most soot and fine aerosols are at altitudes lower than 6 km in this area (Hadley et al., 2007), aerosol scavenging by precipitation should be efficient over the elevated mountains (Fischer et al., 2009). Therefore, we have used the satellite-retrieved AOD as a convenient index to estimate the impact of aerosols on snow albedo in this study.

Gridded precipitation data at a 0.25° resolution was obtained from the U.S. daily precipitation analysis developed by the NOAA Climate Prediction Center using the Modified Cressman Scheme (Glahn, 1985). This dataset did not distinguish rain and snow events. In order to identify snowfall, we have employed atmospheric temperature profiles taken from the MODIS/Terra Level 2 data at a 5 km resolution (Seemann et al., 2003). Approximately 20 vertical profiles within a 0.25 × 0.25° grid of the precipitation data were available for analysis. Since the uncertainties of MODIS temperature profile retrievals are about 3 K (Seemann et al., 2006), we assume that if the temperatures of these profiles at all levels are

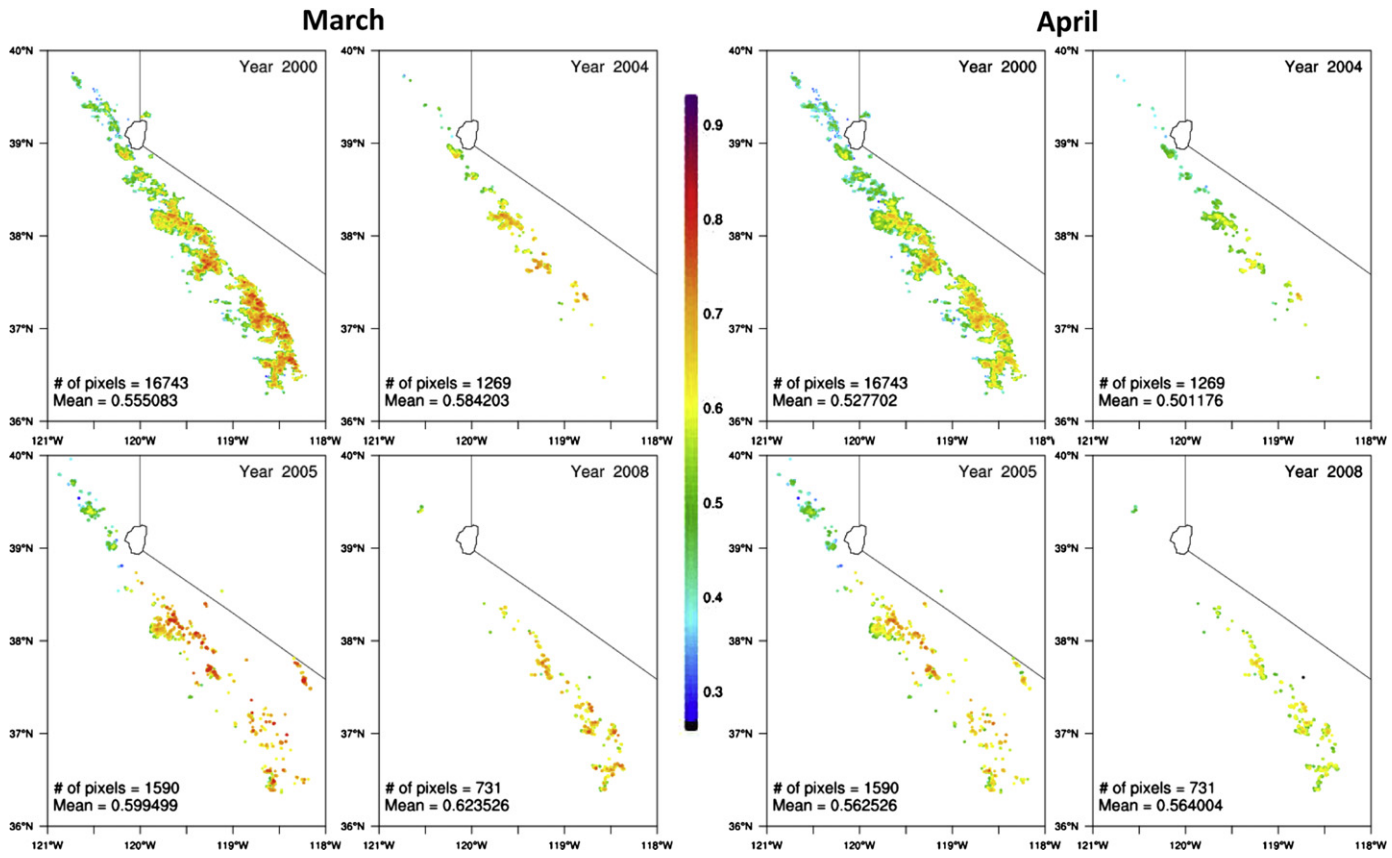

Fig. 2. Surface albedo maps for pixels with 100% snow cover for March (left panels) and April (right panels) for the years 2000, 2004, 2005, and 2008 over the Sierra Nevada region.

less than 270 K when precipitation occurs, this event is considered as snowfall. Because this dataset only contains daily precipitation, the effect of snow aging is quantified in terms of days after each snowfall event (DAS). DAS is defined as zero on the day with snowfall and is equal to 1 for the following day. Therefore, the monthly mean of DAS can be interpreted as the average age of snow grains on the ground.

3. Analysis and discussion

Fig. 3 shows the monthly average of land surface temperature (LST), DAS, AOD, and PSA in the Sierra Nevada region for March and April from 2000 to 2009. The 10-year mean value of PSA is 0.56 with a standard deviation (σ_α) of 0.052. PSA generally decreases from March to April, except in 2003, where PSA is higher in April due to lower surface temperature and more frequent snowfall events. Also, we note that LST, DAS, and AOD are generally larger in April than in March. To investigate the relationship between PSA and LST, AOD, and DAS, we calculate the correlation coefficients using their monthly means for March and April during 2000–2009, that is, there are 20 data points in this analysis, as shown in Fig. 4. The correlation coefficients (r) between PSA and LST, AOD, and DAS are −0.61, −0.42, and −0.07, respectively, implying that LST would have the strongest impact on PSA, followed by AOD and DAS. However, the correlation between DAS and PSA is insignificant at a 90% confidence level.

It is evident that LST, which represents the skin temperature of the snow, and PSA are anti-correlated. A higher temperature would increase the average size of snow grains due to faster coalescence of adjacent grains and faster sublimation for smaller grains than larger ones (Flanner and Zender, 2006). It decreases the total effective surface area of snow grains and subsequently results in snow reflectance reduction. Furthermore, the melting of fresh snow at the top of a snowpack will expose the aged snow underneath, leading to a decrease in PSA. Since a smaller mean DAS implies a more frequent snowfall event, a larger DAS will result in a lower PSA due to more aged snow on the surface. The increase in DAS over the study period represents fewer snowy days in April than in March except in 2003.

Fig. 3 also shows that AOD generally increases from March to April, and this increase is due largely to the fact that more absorbing aerosols have been transported from East Asia by westerlies in April than in March (Liu et al., 2003; Park et al., 2005; Hadley et al., 2007). While only 25% of BC originates from Asia (Verma et al., 2009), Hadley et al. (2010) have shown that the average contribution of Asian dust to the total dust amount in the Sierra Nevada is about 87% in springtime. For example, the AOD reaches maximum in April 2001, corresponding to a massive dust storm originating in the Gobi Desert (Huebert et al., 2003). However, this event did not produce a remarkable albedo reduction, probably because it was simultaneously compensated for by a lower LST and smaller DAS. Other possible explanations for AOD increases during late spring include the increase of moisture during this season, which could produce larger mean aerosol sizes and lead to a larger AOD. Additionally, from March to April in California, the intensification of atmospheric stability traps aerosols in the lower atmosphere, producing a larger AOD. We also found that an increase in AOD is usually accompanied by an increase in DAS with a correlation coefficient of 0.23. It is related to a larger DAS (fewer snowy days) such that fewer aerosols would be washed out from the atmosphere.

Global warming has been recognized as a serious issue on the planetary scale; however, its impact on the regional scale requires more in-depth analysis of observation data. Therefore, we have

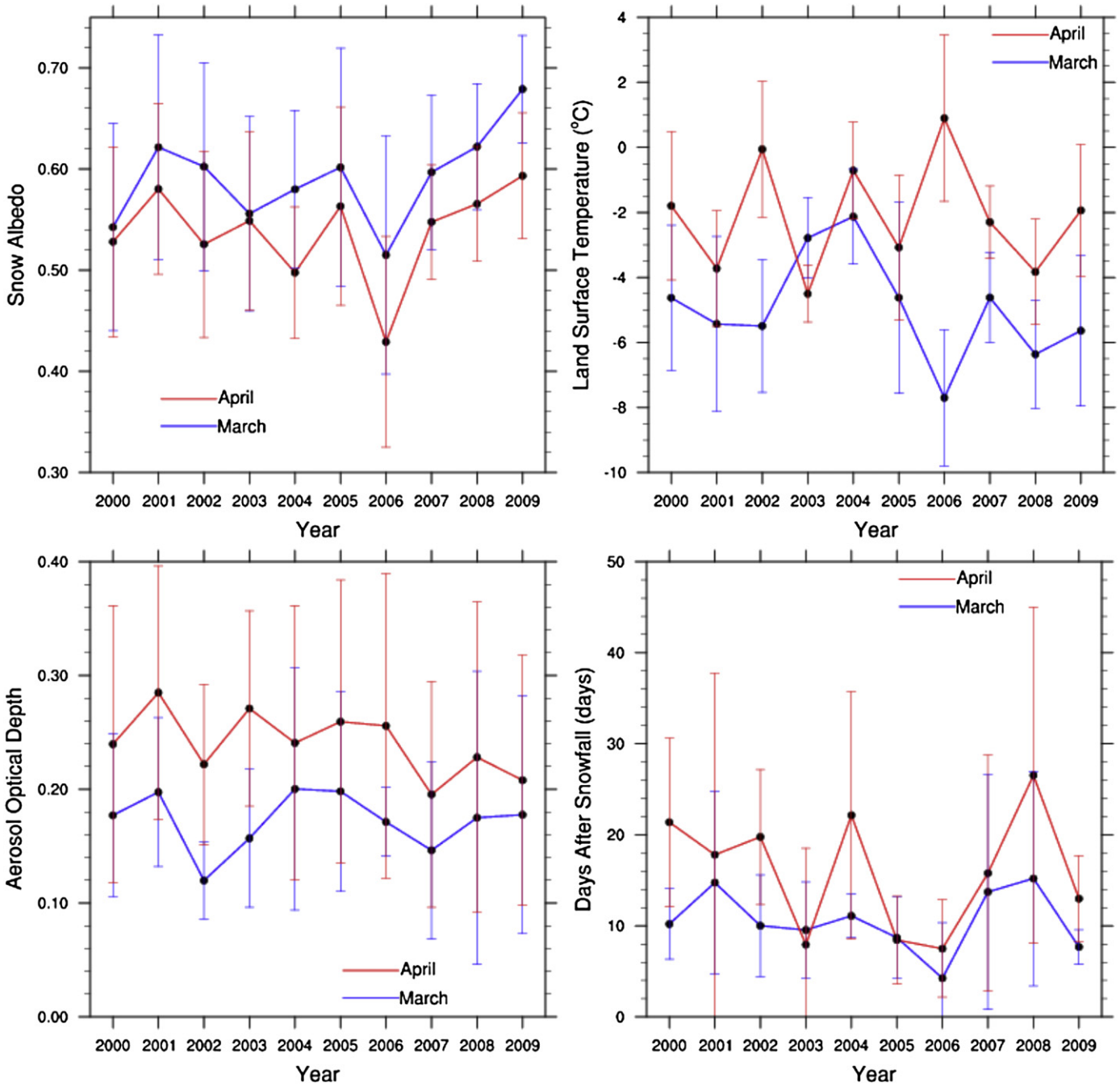

Fig. 3. The monthly averages of snow albedo, land surface temperature, and days after each snowfall event for pixels with 100% snow cover, and aerosol optical depth over the Sierra Nevada in March and April from 2000 to 2009. Error bars indicate one standard deviation.

investigated not only the inter-annual variation in PSA and associated variables, but also their long-term trends. In this study, we found that there is no significant trend for the annual means of PSA and LST for the pixels with 100% snow cover from 2000 to 2009. Furthermore, although it is reported that the number of dust storm occurrences has been decreasing in East Asia due to warming (Zhu et al., 2008) and increased precipitation (Gu et al., 2010) in the Mongolia region, the trend of AOD over the Sierra Nevada is statistically insignificant. It is most likely that a 10-year period may be insufficient to demonstrate a significant trend.

Based on the preceding analysis, LST, AOD, and DAS are not linearly independent. Thus, we employ a multiple linear regression technique to evaluate the relative importance of each parameter on PSA. These parameters were first subtracted by their means (269.6 K, 0.21, and 20.8 days for LST, AOD, and DAS, respectively) and subsequently normalized by their respective standard deviations (2.2 K, 0.041, and 8.3 days for LST, AOD, and DAS, denoted by σ_T, σ_τ, and σ_t, respectively). Multiple linear regression analysis was carried out utilizing these normalized parameters for March and April during the period of 2000–2009; thus, 20 data points for PSA and each parameter were used. As a result, the spatial average of PSA, α, for the pixels with 100% snow cover can be expressed by

$$\alpha = 0.56 - 0.042T - 0.025\tau + 0.009t, \quad (1)$$

where T, τ, and t represent normalized LST, AOD, and DAS, respectively. The multiple correlation coefficient (R^2) has a value of 0.64

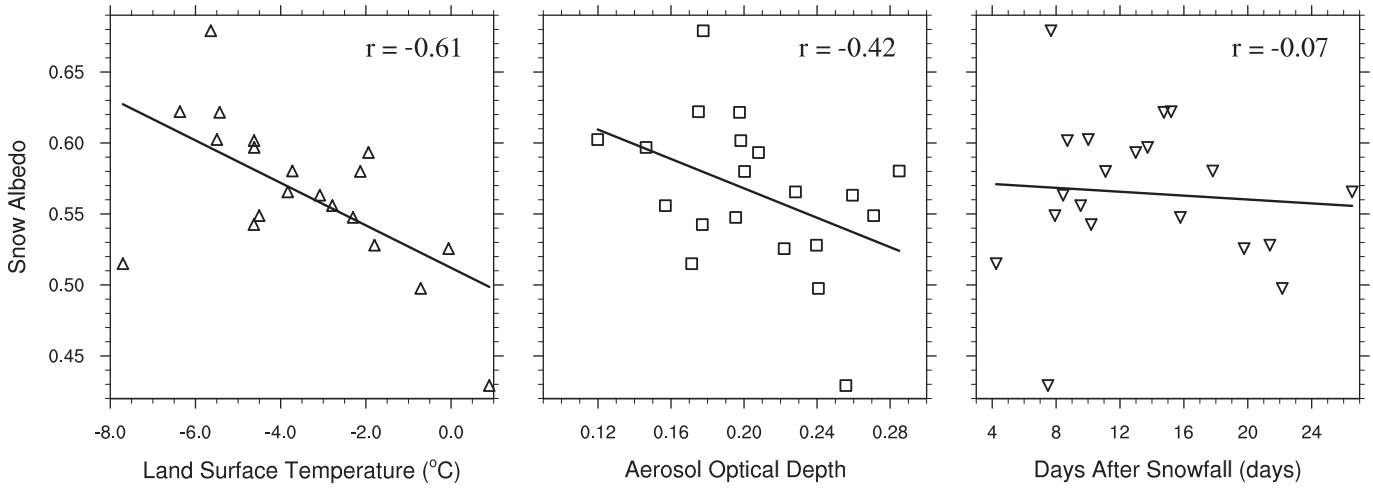

Fig. 4. Regressions of snow albedo against land surface temperature, aerosol optical depth, and days after snowfall, with the correlation coefficients (r) also shown.

with a root mean square error (RMSE) of 0.031, indicating that Eq. (1) can explain 64% of PSA variation.

Eq. (1) shows that a larger DAS will lead to a higher PSA, which contradicts the fact that more aged snow should be darker. Further statistical analysis indicates that the regression coefficient of DAS does not significantly differ from zero at a 90% confidence level, while those for LST and AOD are both significant at a 95% confidence level. The rate of snow aging is proportional to surface temperature as well as contamination of absorbing aerosols. Consequently, the role of DAS on the evolution of PSA is rather indirect when both LST and AOD are accounted for in regression. As shown by Flanner and Zender (2006), the reduction rate of snow albedo might not be a linear function of time. To test the non-linear relation between snow aging, time, and snow temperature, we used the square and square root of DAS, as well as the product of DAS and LST, in regression analysis. The results reveal that all of their regression coefficients in the multiple regression equation are insignificant at a 90% confidence level. Also note that DAS cannot be directly derived from current satellite remote sensing techniques, since precipitation retrieval over land has not been very reliable. On the basis of the preceding reasons, we have removed the effect of DAS from regression.

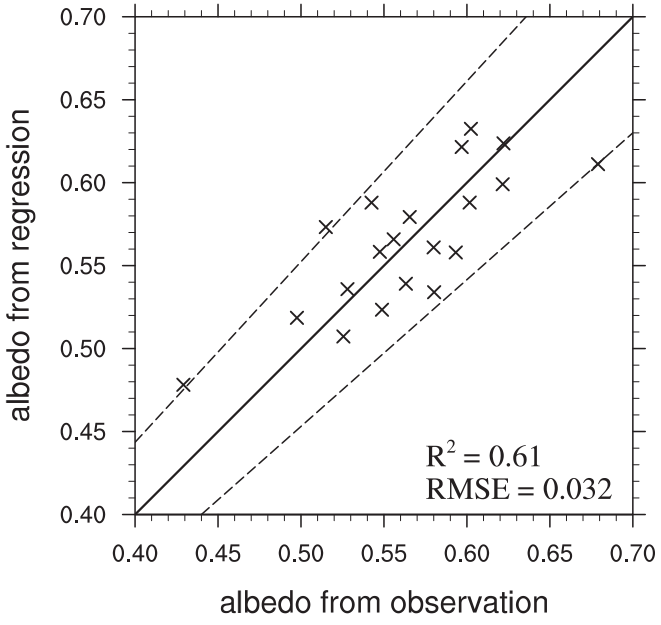

Fig. 5. Comparison of the snow albedo predicted by the regression equation and determined from satellite retrievals. Dashed lines display a 10% relative difference.

When only LST and AOD were taken into account as independent variables in regression analysis, PSA can be expressed by

$$\alpha = 0.56 - 0.038T - 0.026\tau. \quad (2)$$

The multiple correlation coefficient, R^2, has a value of 0.61 with a RMSE of 0.032, illustrating that Eq. (2) can explain 61% of PSA variation. Comparison between observation data and regression results are shown in Fig. 5. The performance of this regression model is reasonably good with relative differences generally within 10%. Eq. (2) shows that if the mean LST reduces by 2.2 K (one σ_T), the average PSA over the Sierra Nevada will increase by 0.038, indicating a gain of $0.76\sigma_\alpha$. Correspondingly, if AOD increases by 0.044 (one σ_τ), PSA will decrease by 0.026, a $0.52\sigma_\alpha$ reduction. If both parameters vary by one standard deviation, the impact of LST on PSA would be larger than AOD, as shown by their respective correlation coefficients.

Using Eq. (2), we can estimate the contributions of LST and AOD to the reduction in PSA from March to April. The LST mean values in March and April are 268.2 K and 271.0 K, respectively, corresponding to a $1.2\sigma_T$ increase from March to April. Furthermore, the AOD mean values in March and April are 0.20 and 0.23, respectively, corresponding to a $0.6\sigma_\tau$ increase from March to April. Eq. (2) predicts that the increases in LST and AOD during this period can lead to reductions in PSA by 0.045 and 0.016, respectively, while the actual mean PSA decreases by 0.055 from March to April. Therefore, approximately 26% of the PSA reduction is contributed by the increase in AOD in springtime.

4. Conclusions

We have investigated the effect of aerosol interception and deposition on snow albedo over the Sierra Nevada in March and April during a 10-year period from 2000 to 2009, from the perspective of satellite remote sensing. To remove the contamination of bare land surfaces, only the pixels with 100% snow cover are selected. In order to clarify the impacts of physical parameters such as snow aging, snow surface temperature, and snow impurities on snow reflectance, we have used the datasets of snow albedo, snow cover, land surface temperature, and aerosol optical depth taken from MODIS. Gridded precipitation analysis data taken from *in situ*

measurements and atmospheric temperature profiles from MODIS have also been used to quantify time after each snowfall event and to distinguish snow from rain.

Snow albedo generally decreases from March to April due to increases in surface temperature and atmospheric aerosol loading, and a decrease in snowfall events. Applying multiple linear regression analysis, the results illustrate that land surface temperature is the most important parameter affecting snow albedo, followed by aerosol optical depth. The days after each snowfall event is statistically insignificant, implying that snow aging is an involved process affected by other parameters such as temperature and snow impurities. The 10-year data show that there are no significant trends for snow albedo, surface temperature, and aerosol optical depth of 100% snow-covered areas over the Sierra Nevada Mountain area. The linear regression model including land surface temperature and aerosol optical depth can explain 61% of the variation in snow albedo over the Sierra Nevada. We show that one standard deviation increases in land surface temperature (2.2 K) and aerosol optical depth (0.044) will lead to decreases in snow albedo by 0.038 and 0.026, respectively. According to the prediction by the regression equation, approximately 26% of the albedo reduction from March to April is contributed by an increase in aerosol optical depth.

Acknowledgments

During the research of this work, K.N. Liou was supported in part by NSF Grant AGS-0946315, while W.-L. Lee was supported by a postdoctoral fellowship at the Academia Sinica.

References

Aoki, T., Hachikubo, A., Hori, M., 2003. Effects of snow physical parameters on shortwave broadband albedos. Journal of Geophysical Research 108 (D19), 4616. doi:10.1029/2003JD003506.

Chylek, P., Ramaswamy, V., Srivastava, V., 1983. Albedo of soot contaminated snow. Journal of Geophysical Research 88, 10837–10843.

Fischer, E.V., Hsu, N.C., Jaffe, D.A., Jeong, M.-J., Gong, S.L., 2009. A decade of dust: asian dust and springtime aerosol load in the U.S. Pacific Northwest. Geophysical Research Letters 36, L03821. doi:20.1029/2008GL036467.

Flanner, M.G., Zender, C.S., 2006. Linking snowpack microphysics and albedo evolution. Journal of Geophysical Research 111, D12208. doi:10.1029/2005JD006834.

Flanner, M.G., Zender, C.S., Randerson, J.T., Rasch, P.J., 2007. Present-day climate forcing and response from black carbon in snow. Journal of Geophysical Research 112, D11202. doi:10.1029/2006JD008003.

Glahn, H.R., 1985. Yes, precipitation forecasts have improved. Bulletin of the American Meteorological Society 66, 820–830.

Gu, Y., Liou, K.N., Chen, W., Liao, H., 2010. Direct climate effect of black carbon in China and its impact on dust storms. Journal of Geophysical Research 115, D00K14. doi:10.1029/2009JD013427.

Hadley, O.L., Ramanathan, V., Carmichael, G.R., Tang, Y., Corrigan, C.E., Roberts, G.C., Mauger, G.S., 2007. Trans-Pacific transport of black carbon and fine aerosols ($D < 2.5$ μm) into North America. Journal of Geophysical Research 112, D05309. doi:10.1029/2006JD007632.

Hadley, O.L., Corrigan, C.E., Kirchstetter, T.W., Cliff, S.S., Ramanathan, V., 2010. Measured black carbon deposition on the Sierra Nevada snow pack and implication for snow pack retreat. Atmospheric Chemistry and Physics 10, 7505–7513.

Hall, D.K., Riggs, G.A., Salomonson, V.V., DiGirolamo, N.E., Bayr, K.A., 2002. MODIS snow-cover products. Remote Sensing of Environment 83, 181–194.

Hall, D.K., Riggs, G.A., Salomonson, V.V., 2012. Updated Daily. MODIS/Terra Snow Cover Daily L3 Global 500m Grid V005, 2000–2009. National Snow and Ice Data Center. Digital media, Boulder, Colorado USA.

Hansen, J., Nazarenko, L., 2004. Soot climate forcing via snow and ice albedos. Proceedings of the National Academy of Sciences 101 (2), 423–428.

Huebert, B.J., Bates, T., Russell, P.B., Shi, G., Kim, Y.J., Kawamura, K., Carmichael, G., Nakajima, T., 2003. An overview of ACE-Asia: strategies for quantifying the relationships between Asian aerosols and their climatic impacts. Journal of Geophysical Research 108, 8633. doi:10.1029/2003JD003550.

Intergovernmental Panel on Climate Change, 2007. In: Solomon, S., Qin, D., Manning, M., Chen, Z., Marquis, M., Averyt, K., Tignor, M., Miller, H. (Eds.), Climate Change 2007: The Physical Science Basis. Cambridge University Press, Cambridge, UK, p. 996.

Jacobson, M.Z., 2007. The Effect of Agriculture and Snow Impurities on Climate and Air Pollution in California. California Energy Commission. PIER Energy-Related Environmental Research Program. CEC-500-2007-022.

Kattelmann, R., 1996. Hydrology and water resources. In: Sierra Nevada Ecosystem Project: Final Report to Congress. Assessments and Scientific Basis for Management Options, vol. II. Centers for Water and Wildland Resources, University of California, Davis, pp. 855–920.

Kim, J., Kim, T., Arritt, R., Miller, N., 2002. Impacts of increased atmospheric CO_2 on the hydroclimate of the western United States. Journal of Climate 15, 1926–1942.

Klein, A.G., Barnett, A.C., 2003. Validation of daily MODIS snow cover maps of the Upper Rio Grande River Basin for the 2000–2001 snow year. Remote Sensing of Environment 86, 162–176.

Klein, A.G., Stroeve, J., 2002. Development and validation of a snow albedo algorithm for the MODIS instrument. Annals of Glaciology 34, 45–52.

Leung, L.R., Ghan, S., 1999. Pacific Northwest climate sensitivity simulated by a regional climate model driven by a GCM. Part II: $2\times CO_2$ simulations. Journal of Climate 12, 2031–2053.

Levy, R.C., Remer, L.A., Mattoo, S., Vermote, E.F., Kaufman, Y.J., 2007. Second-generation operational algorithm: retrieval of aerosol properties over land from inversion of Moderate Resolution Imaging Spectroradiometer spectral reflectance. Journal of Geophysical Research 112, D13211. doi:10.1029/2006JD007811.

Liou, K.N., Takano, Y., Yang, P., 2011. Light absorption and scattering by aggregates: application to black carbon and snow grains. Journal of Quantitative Spectroscopy and Radiative Transfer 112, 1581–1594.

Liu, W., Hopke, P.K., VanCuren, R.A., 2003. Origins of fine aerosol mass in the western United States using positive matrix factorization. Journal of Geophysical Research 108 (D23), 4716. doi:10.1029/2003JD003678.

Marshall, S., Oglesby, R., 1994. An improved snow hydrology for GCMs. Part I: snow cover fraction, albedo, grain size, and age. Climate Dynamics 10, 21–37.

McConnell, J.R., Edwards, R., Kok, G.L., Flanner, M.G., Zender, C.S., Saltzman, E.S., Banta, J.R., Pasteris, D.R., Carter, M.M., Kahl, J.D.W., 2007. 20th-century industrial black carbon emissions altered arctic climate forcing. Science 317, 1381–1384.

Ming, J., Xiao, C., Cachier, H., Qing, D., Qin, X., Li, Z., Pu, J., 2009. Black Carbon (BC) in the snow of glaciers in west China and its potential effects on albedos. Atmospheric Research 92, 114–123.

Park, R.J., Jacob, D.J., Palmer, P.I., Clarke, A.D., Weber, R.J., Zondlo, M.A., Eisele, F.L., Bandy, A.R., Thornton, D.C., Sachse, G.W., Bond, T.C., 2005. Export efficiency of black carbon aerosol in continental outflow: global implications. Journal of Geophysical Research 110, D11205. doi:10.1029/2004JD005432.

Pu, Z., Xu, L., Salomonson, V., 2007. MODIS/Terra observed seasonal variations of snow cover over the Tibetan Plateau. Geophysical Research Letters 34, L06706. doi:10.1029/2007GL029262.

Riggs, G.A., Hall, D.K., Salomonson, V.V., 2006. MODIS Snow Products User Guide. http://modis-snow-ice.gsfc.nasa.gov/sugkc2.html.

Seemann, S.W., Li, J., Menzel, W.P., Gumley, L.E., 2003. Operational retrieval of atmospheric temperature, moisture, and ozone from MODIS infrared radiances. Journal of Applied Meteorology 42, 1072–1091.

Seemann, S.W., Borbas, E.E., Li, J., Menzel, W.P., Gumley, L.E., 2006. MODIS Atmospheric Profile Retrieval Algorithm Theoretical Basis Document. Version 6. Univ. Wisconsin-Madison.

Stamnes, K., Tsay, S.C., Wiscombe, W., Jayaweera, K., 1988. Numerically stable algorithm for discrete-ordinate-method radiative transfer in multiple scattering and emitting layered media. Applied Optics 27 (12), 2502–2509.

VanCuren, R.A., Cliff, S.S., Perry, K.D., Jimenez-Cruz, M., 2005. Asian continental aerosol persistence above the marine boundary layer over the eastern North Pacific: continuous measurements from Intercontinental Transport and Chemical Transformation 2002 (ITCT 2K2). Journal of Geophysical Research 110, D09S90. doi:10.1029/2004JD004973.

VanCuren, R.A., 2003. Asian aerosols in North America: extracting the chemical composition and mass concentration of the Asian continental aerosol plume from long-term aerosol records in North America: frequency and concentration of fine dust. Journal of Geophysical Research 108 (D20), 4623. doi:10.1029/2003JD003459.

Verma, S., Worden, J., Payra, S., Jourdain, L., Shim, C., 2009. Charactering the long-range transport of black carbon aerosols during transport and chemical evolution over the pacific (TRACE-P) experiment. Environmental Monitoring and Assessment 141, 85–92. doi:10.1007/s10661-008-0379-2.

Wan, Z., 2012. Updated Daily. MODIS/Aqua Land Surface Temperature/Emissivity Daily L3 Global 0.05Deg CMG, 2000–2009. EDC LPDAAC, Sioux Falls, South Dakota, USA. Digital media.

Warren, S., Wiscombe, W., 1980. A model for the spectral albedo of snow. II: snow containing atmospheric aerosols. Journal of Atmospheric Sciences 37, 2734–2745.

Zhu, C., Wang, B., Qian, W., 2008. Why do dust storms decrease in northern China concurrently with the recent global warming? Geophysical Research Letters 35, L18702. doi:10.1029/2008GL034886.